Proceedings of ISFOG 2025
5TH INTERNATIONAL SYMPOSIUM ON
FRONTIERS IN OFFSHORE GEOTECHNICS
Nantes, France | June 9-13 2025

ISBN 978-2-85782-758-0

Shear Plane Analysis of Deployable Anchors and Insights from X-ray Microtomography

Elizabeth Capretta (ec36@illinois.edu)
University of Illinois Urbana-Champaign, Urbana, United States
Khuzaima Hummad (hummad2@illinois.edu)
University of Illinois Urbana-Champaign, Urbana, United States
*S M Shazeebur Rahman *(*srahman049@vt.edu)*
Virginia Polytechnic Institute and State University, Blacksburg, United States
Ryan D Beemer(*rbeemer@vt.edu*)
Virginia Polytechnic Institute and State University, Blacksburg, United States
Ann C Sychterz (asychter@illinois.edu)
University of Illinois Urbana-Champaign, Urbana, United States

ABSTRACT: This paper investigates the behavior of deployable anchors using plane strain and X-ray microtomography (μCT) experiments. A deployable structure is a system that changes size and shape under applied loads, presenting a novel approach to reduce transportation and life cycle costs of materials without sacrificing load-carrying capacity. Presented is the experimental methodology to determine the increase in the shear plane in sandy soil using deployable underground anchors. Ink tacking technique was employed to locate the shear plane. This study finds that the ink tracking technique captures the shear plane effects in sandy soil for deployable awns in ground anchors. Moreover, bar cross-section optimization represents origami behavior under in-plane and out of plane loading. In addition, the initial results of the deployable geosystem - soil interaction from μCT are presented. Experimental testing involves subjecting a scale model deployable system to displacement-controlled loading in sand. Utilizing μCT scanning with 35 μm voxels, images are captured to track the bending of the anchor's awns (compliant appendages).
Keywords: Deployable anchor; X-ray microtomography; Particle movement; Shear Plane.

1 INTRODUCTION

Traditional cylindrical pile anchors are usually designed based on the interaction between the pile's surface area and the surrounding soil, as this interaction determines the pull-out capacity (Aubeny 2017). Consequently, cylindrical piles tend to be over-designed, using more material than strictly necessary to meet strength requirements. The installation of underground piles, typically through using impact or vibration hammers, induces vibrations in the surrounding soil, and poses potential harm to nearby existing structures or equipment (Colaço et al. 2021). To address these challenges, deployable structures are proposed, aiming to be a materially efficient design that has less significant effects on nearby structures. This novel design features a pile with deployable attachments, referred to as awns. This design can maintain an equivalent surface area to cylindrical piles while using less material due to the deployable awn attachments. Furthermore, this design utilizes a torque-driven installation process, similar to the installation process for helical anchors, rather than using impact or vibration hammers. The shear plane effects of these deployable awns in sandy soil have yet to be experimentally explored, and an equivalent model of these awns has yet to be computationally analyzed.

Within the field of geotechnical engineering, there have been studies that explore geotechnical systems that deploy during installation such as suction embedded plate anchors and piles with anchor wings (Wilde et al. 2001, Aubeny 2017, Sakr et al. 2020). Concurrently, experimental investigations have explored the effects of soil disturbance during the installation of helical piles on their tensile capacity (Lutenegger and Tsuha 2015). Large scale field tests have also been performed to study the soil disturbance effects associated with the drilling of tie back anchors (Kempfert and Gebreselassie 1999, Lande et al. 2020). However, an analysis of the shear plane in sandy soil, resulting from the installation of the deployable ground anchor, remains unexplored.

Inspired by Japanese paper folding, origami structures use folding patterns to create lightweight, deployable, and kinematically stable load-bearing systems with high structural efficiency. These structures have successfully been modeled using bar-and-hinge models (Filipov et al. 2017). Previous work by authors modeled origami as bar-and-hinge models by modeling the creases as hinges and the panels in between the creases as rigid links (Sychterz and Baruah 2021, Baruah and Sychterz 2022). Bar-and-hinge models have yet to be used for modeling the deployable awn attachments on underground deployable anchors.

X-ray micro-computed tomography (μCT) is a powerful non-destructive imaging technique increasingly used to explore the structural properties of soils in three dimensions. In μCT, a series of 2D radiographs is captured from various angles and then reconstructed to form a 3D model (Viggiani et al., 2015). This unique technique enables changes in soil structure under stress to be captured without disturbing the sample, which is critical for observing processes like strain localization (Desrues et al., 2006; Peth et al., 2010), pore collapse (Pires et al., 2020), and the formation of failure planes (Paniagua et al., 2013; Stefaniuk et al., 2015).

The first objective of this paper is to develop a simple ink tracking technique to measure the shear plane location that results from the deployment of underground deployable anchors in a plane strain configuration and to model the deployable awn attachments as bar-and-hinge models. The second is to demonstrate the feasibility of using X-ray microtomography μCT to visualize deployable geosystems deformation in three-dimensional experiments.

2 INK TRACKING DOT INVESTIGATION

The ink dot tracking method is an experimental technique used to visualize and analyze deformation, displacement, and shear behavior in granular materials. This was developed as a simplified method compared to (Sadek et al., 2003; Stanier et al., 2016; White et al., 2003) for measuring soil movements in plain strain structure topology optimization experiments. A setup was constructed to deploy the anchor while recording the sand displacement data. A representation of the test set up can be seen in Figure 1. A similar test set up was used previously in this lab, using the same materials (Tucker and Sychterz 2022). A clear acrylic box with dimensions 14.6 cm x 14.6 cm x 4.76 cm sat on an elevated wooden crate. Below the crate was a camera to capture the bottom of the box acrylic box as the anchor was deployed. Two pieces of wood were clamped beside to the acrylic box to prevent the box from shifting during the tests. Pulley clamps were attached to the edges of the crate and were aligned with the center of the acrylic box.

Gel food coloring was mixed with water in a 1:1 ratio to create a concentrated ink mixture. Dots of ink were added in a grid formation at the bottom of the acrylic box, at a spacing of 6.35 mm, as shown in Figure 1b. The main shaft of the anchor has a diameter of 25 mm and a height of 75mm and was printed with the 3D printing acrylic material called VeroMagentaV. The awns of the ground anchor had a height of 25 mm, and the thickness of the awn was tapered to the circumference of the anchor, with the largest thickness being 2.0 mm. The material of the 3D-printed awns was a mix of VeroMagenta and rubber material called Agilus. The petroleum jelly helped keep the deployable anchor in place during the test set up, and to ensure that the anchor deployed smoothly without sand underneath the pile.

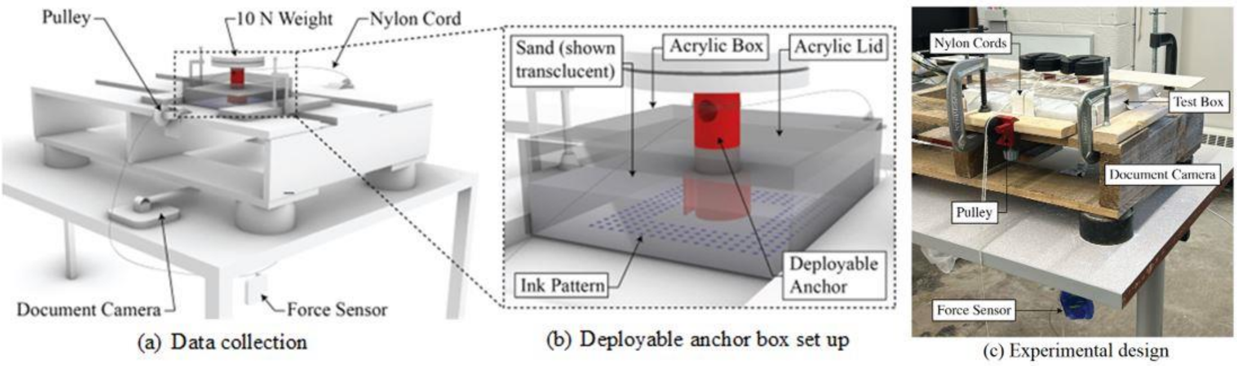

Figure 1.Test Set Up Representation

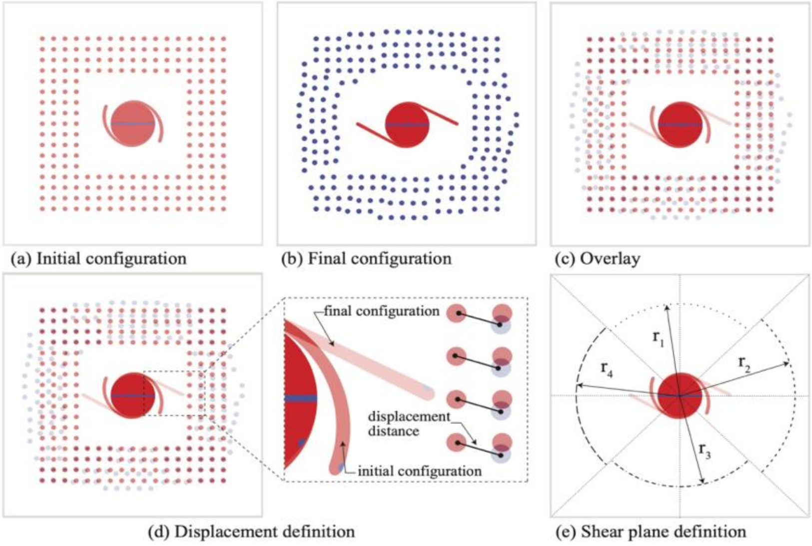

Figure 2. Ink Tracking Technique

Once the ink pattern was added to the bottom of the acrylic box and the anchor was placed in the center of the box, fused silica sand was added into the acrylic box up to a 25 mm mark to ensure the awns were covered. To ensure the deployable anchor remained centered during testing, an acrylic lid with a hole for the anchor pile was placed near the top of the acrylic box. This also allowed sand to move over the awns as they deployed. A nylon string was threaded through the hole at the top of the pile, wrapped counterclockwise around it, guided across pulleys on the wooden crate's sides, and tied beneath the table. During the test, the nylon cord was pulled to deploy the anchor 180 degrees. A force sensor was attached to the nylon cord beneath the table to record the applied force. Additionally, a 10 N weight was placed on top of the ground anchor to ensure the deployable anchor did not lift out of the acrylic box during the test. The movement of the ink pattern on the bottom of the test set up box is recorded by the document camera beneath the box during deployment. The displacement of the ink dots is used to determine the location of the shear plane that results from the deployment of the awns. The methodology that is developed is described in the results section of this paper. To analyze the computational structural behavior of a single awn, an equivalent representation of the awn was created in the form of a bar and hinge truss model. By matching the deformations of the bar and hinge model to the deformation of the awn, the model was created.

This model is developed to represent the awns protruding from the pile to quantify the in-plane and out-of-plane deformation behavior and equivalent stiffness between the computational finite element model and bar-and-hinge model. Prior to applying external loads, the awns are analyzed to calculate the in-plane and out of plane deformation characteristics under different boundary conditions, specifically pinned and roller supports. The loads are distributed across the end node. To form the bar and hinge model, the bar elements are sized to match the overall geometry of the awn plate so that the bar model has the same planar dimensions as the awn (25 mm x 25 mm). To determine the individual bar diameters, the total volume in the awn plate is equated to the combined volume in all the circular bars, by

$$D_b = 2\sqrt{\frac{V_a}{\pi L_b}}$$

where D_b is the new bar diameter, V_a is the volume of the awn, and L_b is the length of the bars.

This establishes an initial proportional size estimate across the various truss elements. The out-of-plane deformation with the new diameter is re-calculated and compared to the experimental awn deformation. Calculating the tuned diameters from the out-of-plane analysis, the bar model is further assessed for in-plane deformations. Both the longitudinal and lateral axial deformations are quantified under loading. These results are compared to the awn deformation. If the bar-in-plane deformations match within 10% error margin, the model sufficiently represents an equivalent simulation of the awn. If deviations exceed 10%, the iterative diameter tuning process is repeated, and the iteration repeats until there is a deformation of the bar-and-hinge model within 10% error of the deformation of the awn.

To find the shear plane location due to the deployment of the ground anchor, an ink spread tracking technique was developed. First, two images must be taken from the recording of the deployment test. The first image is the initial configuration before deployment, Figure 2a, and the second image is the final configuration after the deployment of the ground anchor, Figure 2b. The initial configuration image is overlaid on the final configuration to create the overlay image that will be analyzed, Figure 2c. The image is then divided into eight sections, and the displacement of the ink dots is defined as shown in Figure 2d. Finally, the eight radius values were grouped and averaged to determine the four shear plane radius values depicted in Figure 2e. The shear plane radius values r1 and r2 result from the deployment of one awn, and the radius values r3 and r4 result from the deployment of the second awn.

3. X-RAY MICROTOMOGRAPHY INVESTIGATION

Since the Ink Tracking Method or any similar techniques are limited to plane strain analysis against a transparent surface, an initial investigation into the use of μCT analysis was completed on a simple T-shaped deployable geosystem tested in axial loading. The T of the deployable system had dimension of 40 mm by 10 mm by 1.0 mm and the shaft had a diameter of 6.0 mm (Figure 3). Tests were conducted in a 60 mm diameter container with a silica sand. The boundaries of this container will affect the movement of the soil particles but due to the constrains of X-ray field of view and image resolution the experiment is set this way to gather images which will help understanding the deployable awn- soil interaction. Index properties of the sand were not collected at this initial proof of concept stage. The experiments were conducted under displacement control loading in six total increments of 1 mm. At each step the experiment was scanned with the Zeiss Xradia versa-610 x-ray microscope at a resolution of 35 μm per voxel. Each scan took on the order of eight hours to complete. Output from the μCT device was converted to tif images for each position using ImageJ (Schneider et al., 2012) with the XRM Reader plug in (Sutherland M, 2017). The tif images were then loaded into MATLAB R2024b and the center slices were taken for analysis (Figure 4). From this study it can be seen that the μCT can be used to visualize the deformation of a deployable geosystem in a silica soil under displacement-controlled loading. Interesting stress arching appears apparent ahead of the awn with a gap forming under the T-shaped (Red zone in Figure 4). The μCT scans further highlight how soil particles adjust and rearrange to accommodate the imposed load, resulting in localized void redistribution near the edges of the anchor and the surrounding stress zones.

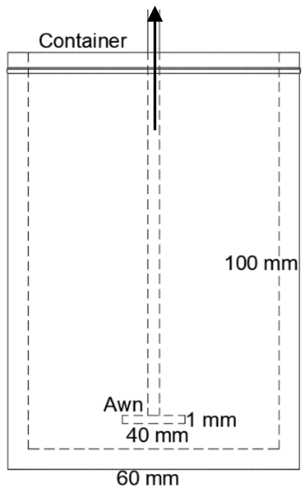

Figure 3. X-Ray container with awn

4. CONCLUSIONS

The ink tracking technique presented in this paper is an effective method for experimentally determining the location of the shear plane in sandy soil from the deployment of the awns of the ground anchor systems. In addition, the equivalent bar area for the thick origami in the bar-and-hinge model was successful in characterizing the in-plane and out-of-plane behavior of the deployable awns. These understandings of how to experimentally analyze and computationally replicate the behavior of the deployable ground anchors are useful techniques that can help in the development of future designs of the deployable anchors.

The investigation demostrates that it is feasible to study deployable systems fully embedded in silica sand using μCT. It highlights the significance of stress arching and void redistribution related to grain scaling in these types of tests. Specifically, stress arching was observed ahead of the awn, while void formation beneath the T-shaped anchor became more pronounced with increasing displacement. This underscores the importance of considering particle-scale interactions and stress redistribution in the design and analysis of deployable systems.

AUTHOR CONTRIBUTION STATEMENT

Elizabeth Capretta Data curation, Formal Analysis, Writing- Original draft. **Khuzaima Hummad** Data curation, Formal Analysis, Writing- Original draft.

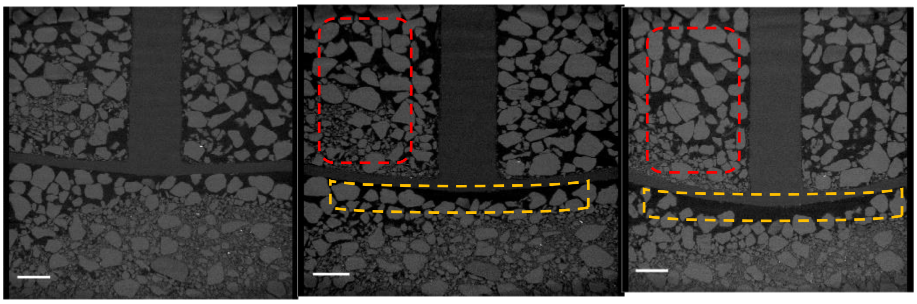

Figure 4. Deployable anchor visualization from μCT under vertical displacement control loading. Position 1- zero displacement (left) Position 3- 2 mm displacement (middle), and Position 6- 5 mm Displacement (right). Bar is 6 mm and images were digital brightened for ease of visualization

S M Shazeebur Rahman Investigation, Writing, Editing. **Ryan Beemer**: Supervision, Writing-Reviewing and Editing. **Ann Sychterz**: Supervision, Funding acquisition, Writing- Reviewing and Editing.

ACKNOWLEDGEMENTS

The authors are grateful for the financial support provided by The National Science Foundation (NSF) Engineering Civil Infrastructure CMMI-2348959.

REFERENCES

Aubeny, C. (2017). Geomechanics of marine anchors. CRC Press. https://doi.org/10.4324/9781351237376

Baruah, A. C., & Sychterz, A. C. (2022). Assessment and Comparison of Cable-Actuation of Pill Bug Inspired Adaptive Origami Structure Using Computer Vision and Dynamic Relaxation. Frontiers in Built Environment, 8, 813543. https://doi.org/10.3389/fbuil.2022.813543

Colaço, A., Costa, P. A., Parente, C. M. A., & Cardoso, A. S. (2021). Ground-borne noise and vibrations in buildings induced by pile driving: An integrated approach. Applied Acoustics, 179, 10805. https://doi.org/10.1016/j.apacoust.2021.108059

Desrues, J., Viggiani, G., & Besuelle, P. (Eds.). (2006). Advances in X-ray tomography for geomaterials. GeoX 2006, London; Newport Beach, CA. ISTE.

Filipov, E. T., Liu, K., Tachi, T., Schenk, M., & Paulino, G. H. (2017). Bar and hinge models for scalable analysis of origami. International Journal of Solids and Structures, 124, 26-45. https://doi.org/10.1016/j.ijsolstr.2017.05.028

Kempfert, H. G., & Gebreselassie, B. (1999, July). Effect of anchor installation on settlement of nearby structures in soft soils. In Proceedings international symposium On Geotechnical Aspects of Underground Construction in Soft Ground, IS-Tokyo (Vol. 99, pp. 19-21).

Lande, E. J., Karlsrud, K., Langford, J., & Nordal, S. (2020). Effects of drilling for tieback anchors on surrounding ground: Results from field tests. Journal of Geotechnical and Geoenvironmental Engineering, 146(8), 05020007. https://doi.org/10.1061/(ASCE)GT.1943-5606.0002274

Lawrence, P. L. (1994). Natural hazards of shoreline bluff erosion: a case study of Horizon View, Lake Huron. Geomorphology, 10(1-4), 65-81. https://doi.org/10.1016/0169-555X(94)90008-6

Levine, K. J., Jahn, N. T., Kotz, E., & Roscizewski, A. (2020). What do our lakes mean to us? An understanding of Michigan coastline communities' perceptions of the Great Lakes. Journal of Great Lakes Research, 46(6), 1716. https://doi.org/10.1016/j.jglr.2020.09.001

Lutenegger, A. J., & Tsuha, C. D. H. (2015, December). Evaluating installation disturbance from helical piles and anchors using compression and tension tests. In Proceedings of the 15th Pan-American Conference on Soil Mechanics and Geotechnical Engineering, Buenos Aires, Argentina (pp. 373-381). Press. http://dx.doi.org/10.3233/978-1-61499-603-3-373

Paniagua, P., Andò, E., Silva, M., Emdal, A., Nordal, S., & Viggiani, G. (2013). Soil deformation around a penetrating cone in silt. Géotechnique Letters, 3(4), 185–191. https://doi.org/10.1680/geolett.13.00067

Peth, S., Nellesen, J., Fischer, G., & Horn, R. (2010). Non-invasive 3D analysis of local soil deformation under mechanical and hydraulic stresses by μCT and digital image correlation. Soil and Tillage Research, 111(1), 3–18. https://doi.org/10.1016/j.still.2010.02.007

Pires, L. F., Auler, A. C., Roque, W. L., & Mooney, S. J. (2020). X-ray microtomography analysis of soil pore structure dynamics under wetting and drying cycles. Geoderma, 362, 114103. https://doi.org/10.1016/j.geoderma.2019.114103

Poulos, H. G. (1995). Design of reinforcing piles to increase slope stability. Canadian Geotechnical Journal, 32(5), 808-818. https://doi.org/10.1139/t95-078

Sadek, S., Iskander, M. G., & Liu, J. (2003). Accuracy of Digital Image Correlation for Measuring Deformations in Transparent Media. Journal of Computing in Civil Engineering, 17(2), 88–96. https://doi.org/10.1061/(ASCE)0887-3801(2003)17:2(88)

Sakr, M., Nazir, A., Azzam, W., & Sallam, A. (2020). Model study of single pile with wings under uplift loads. Applied Ocean Research, 100, 102187. https://doi.org/10.1016/j.apor.2020.102187

Schneider, C. A., Rasband, W. S., & Eliceiri, K. W. (2012). NIH Image to ImageJ: 25 years of image analysis. Nature Methods, 9(7), 671–675. https://doi.org/10.1038/nmeth.2089

Stanier, S. A., Blaber, J., Take, W. A., & White, D. J. (2016). Improved image-based deformation measurement for geotechnical applications. Canadian Geotechnical Journal, 53(5), 727–739. https://doi.org/10.1139/cgj-2015-0253

Stefaniuk, D., Tankiewicz, M., & Stróżyk, J. (2015). X-Ray Microtomography (μCT) as a Useful Tool for Visualization and Interpretation of Shear Strength Test Results. Studia Geotechnica et Mechanica, 36(4), 47–55. https://doi.org/10.2478/sgem-2014-0035

Sutherland, M., (2017). Maven project implementing an ImageJ 1.x plugin to load TXM files. https://github.com/mrsutherland/XRM_Reader.

Sychterz, A. C., & Baruah, A. C. (2021). Active control for adaptive origami structures undergoing damage. Engineering Structures, 242, 112457. https://doi.org/10.1016/j.engstruct.2021.112457

Tucker, K. A., & Sychterz, A. C. (2022, May). Analyzing Geosystems with Deployable Compliant Mechanisms for Enhanced Tension Capacity. In Canadian Society of Civil Engineering Annual Conference (pp. 483-494). Cham: Springer Nature Switzerland.

Viggiani, G., Andò, E., Takano, D., & Santamarina, J. C. (2015). Laboratory X-ray Tomography: A Valuable Experimental Tool for Revealing Processes in Soils. Geotechnical Testing Journal. https://doi.org/10.1520/GTJ20140060

Volpano, C. A., Zoet, L. K., Rawling III, J. E., Theuerkauf, E. J., & Krueger, R. (2020). Three-dimensional bluff evolution in response to seasonal fluctuations in Great Lakes water levels. Journal of Great Lakes Research, 46(6), 1533-1543. https://doi.org/10.1016/j.jglr.2020.08.017

White, D. J., Take, W. A., & Bolton, M. D. (2003). Soil deformation measurement using particle image velocimetry (PIV) and photogrammetry. Géotechnique, 53(7), 619–631. https://doi.org/10.1680/geot.2003.53.7.619

Wilde, B., Treu, H., & Fulton, T. (2001, June). Field testing of suction embedded plate anchors. International Ocean and Polar Engineering Conference (pp. ISOPE-I). ISOPE.